A numerical study on the effects of exhaust locations on energy consumption and thermal environment in an office room served by displacement ventilation

Ahmed Qasim Ahmed*, Shian Gao, Ali Khaleel Kareem

Department of Engineering, University of Leicester, Leicester LE1 7RH, United Kingdom

*Corresponding author: phone: +44(0)116 252 2874; fax: +44(0)116 252 2525; e-mail: aqaa2@ le.ac.uk.

ABSTRACT

In an office room, many factors affect the pattern of airflow, thermal comfort, indoor air quality and energy saving. In this study, the effects of the location of exhaust diffusers where the warm and contaminant air is extracted and their relation to room heat sources on thermal comfort and energy saving were investigated numerically for an office served by a displacement ventilation system. The indoor air quality in the breathing level and the inhaled zone were also evaluated. The contaminants were released from window and door frames in order to simulate the contaminants coming from outside. The amount of energy consumption and the indoor thermal environment for various exhaust locations were investigated numerically using the computational fluid dynamics techniques. The results showed that the thermal indoor environment, thermal comfort, quality of indoor air and energy saving were greatly improved by combining the exhaust outlets with some of the room's heat sources such as ceiling lamps and external walls. In particular, a 25.0 % of energy saving was achieved by combining the exhaust diffuser with room's ceiling lamps. In addition, locating the exhaust diffuser near the heat sources also reduced the cooling coil load by 13.8 %. The risk of a large difference in temperature between the head and foot levels, increased particle concentration in the occupied zone, as well as increased energy consumption was also clearly demonstrated when the exhaust and recirculated air outlet (return opening) were combined in one unit in the occupied boundary area that

is located at 2m away from the occupants. Thus, for the optimum energy saving and better indoor environment, the combination of the indoor heat sources with the exhaust outlet is necessary.

Key words: Energy saving, Thermal comfort, Indoor air quality, Displacement ventilation, Contaminant removal

Nomenclature

Abbreviations

DV	displacement ventilation
HVAC	heating, ventilation and air conditioning system
IAQ	indoor air quality
PMV	predicted mean vote
PPD	predicted percentage of dissatisfied
STRAD	stratified air distribution system

Latin letters

C	the mean particle concentration (kg/m^3)
$C_{1\varepsilon}$, $C_{2\varepsilon}$	model constants in the term ε of the turbulence model
C_n	the normalised concentration.
C_p	the contaminant concentration in a specific region (kg/m^3)
C_e	the concentration at exhaust (kg/m^3)
C_μ	model constant of the turbulence model
c_p	specific heat of air (J/(kg k)
d_p	particle diameter (m)
dt	particle residence time
F_D	inverse of relaxation time(s^{-1})
$\vec{F}_a$	force acting on particle (m/s^2)
$\vec{F}_b$	the Brownian force (m/s^2)
$\vec{F}_{thermal}$	the thermophoretic force (m/s^2)
$\vec{F}_s$	the Saffman's lift forces (m/s^2)
$\vec{g}$	gravitational acceleration (m/s^2)
i	trajectory index
j	cell index
k	turbulent kinetic energy per unit mass (J/kg)
$\dot{m}$	mass flow rate associated with each trajectory (kg/s)
$\dot{m}_e$	the exhaust mass flow rate (kg/s)
n	trajectory number
P_k	additional term in the turbulence model
$Q_{coil-STRAD}$	the cooling coil load for the STRAD system (W)
Q_{space}	the cooling coil load of space (W)
Q_{vent}	the ventilation load (W)
$Q_{coil-MV}$	the cooling coil load for the mixing ventilation system (W)
S	mean strain rate tensor magnitude
S_{ij}	strain rate tensor
T_e	the exhaust temperature (℃)
T_{set}	room set temperature (℃)
t	time (s)
$\vec{u}_p$	particle velocity vector (m/s)
u	fluid velocity (m/s)
u_i'	fluctuating velocity (m/s)
V_j	volume associated with i trajectory and cell j

Greek letters

β	coefficient of thermal expansion (1/K)
ε	turbulent dissipation rate (m^2/s^3)
λ	represents the molecular mean free path
μ	dynamic viscosity (kg/(m s)
ξ_i	the normally distributed random number
ρ	fluid density (kg/m^3)
ρ_p	particle density (kg/m^3)
σ_k	model constant for k equation of the turbulence model
σ_ε	model constant for ε equation of the turbulence model

1. Introduction

One of the most important aims of the Heating, Ventilation and Air Conditioning (HVAC) system is to create a healthy and comfortable environment and reduce indoor contaminant concentration. An efficient design of HVAC system requires the proper placement of the supply and exhaust outlet with respect to a room's geometry configuration, distribution of indoor heat sources and indoor thermal conditions [1-3]. With the increase of the energy used for improving the quality of the indoor environment [4-6], there is a requirement to use effective ventilation strategies [7-9], while maintaining acceptable indoor thermal environment. In most air distribution systems, the ventilation performance and energy saving are greatly influenced by the arrangements of the supply, return and exhaust diffuser positions. Awad et al. [10] conducted experiments to investigate air flow patterns and velocity distribution using different exhaust diffuser locations. Their results indicated that the exhaust diffuser's position had a great impact on the level of the thermal stratification layers which consequently affected the cooling coil load. Cheng et al. [11] reported that a 20.8% of energy saving was achieved when the supply inlet located at the floor level and the return outlet located at occupied level. They also found that, the energy saving and indoor thermal comfort were improved by distributing the supply diffuser in the occupied zone. Bagheri and Gorton [12] investigated the relationship between the return outlet location and cooling load. They concluded that extra energy saving can be achieved by positioning the return vent in the cooled zone near the floor. Filler [13] reported that energy saving can be improved by placing the return vent near the perimeter walls of the room where the convective heat flux will be extracted directly by means of the return vent before mixing with the air in the occupied zone. Hongtao et al. [14] found that extra energy saving can be achieved by separating the exhaust and return vent in two different elevations.

Thermal plumes generated from occupants and indoor heat sources play a significant role in increasing the exposure level for the occupants in the breathing zone by transporting the particles from floor level towards the upper part of the room, passing through the occupant inhaled area [15]. Therefore, the arrangement of the heat sources in a room may play an important role in the room's air flow pattern, thermal comfort, contaminant distribution and energy saving [16]. Park and Holland [17] investigated the effect of heat source positions on thermal stratification in a room served by a displacement ventilation (DV) system. They reported that indoor thermal environment and energy consumption are significantly influenced by changing the positions of the room's heat sources, and they also found that by increasing the height of heat source location the convective heat becomes less significant. Cheng et al. [18] performed the experimental and numerical study in a room chamber to investigate the influences of changing return opening on both thermal comfort and energy saving. In their experiments, the combination between the lamps and some exhaust opening was used. Further investigation of the combination between the lamps and exhaust opening was performed by the authors [19]. In this publication, the impact of the combination between the room lamps and exhaust opening on the energy saving was investigated numerically. The results showed that extra energy saving can be achieved in rooms that had combined the exhaust with lamps into one unit.

Safer thermal environmental conditions can be achieved in terms of contaminant distribution when using the exhaust vent at the upper part and the supply diffuser at the low part of the room [20]. The influences of the supply and exhaust locations of diffusers were numerically investigated by Khan et al. [21]. Their results showed that a better indoor air quality (IAQ) was achieved by locating the exhaust opening near the ceiling level. Kuo and Chung [22] investigated the impact of supply and outlet diffuser positions on indoor thermal comfort in the occupied zone using different ventilation strategies. Based on their simulation

results, they found that the longer the supply air throw in the occupied region is, the better the indoor thermal comfort achieved. He et al. [1] reported that the exhaust vent position may not greatly influence the pattern of airflow, but it can significantly affect the indoor exposure level. Lin et al. [23] studied the impact of the position of the supply diffusers on the DV system performance. They revealed that for a better indoor environment the supply opening should be located close to the room centre.

Most previous studies have investigated the effect of the supply and return diffuser's locations on the performance of a ventilation system, thermal comfort, IAQ and energy saving. But limited research has been performed to investigate the relationship between the location of the exhaust outlet diffuser and the heat sources in a room. The thermal plumes of the indoor heat source and the exhaust temperature play a significant role in indoor contaminant transport and energy saving respectively [13, 24]. In this study, a validated CFD model was used to investigate the effect of different locations of the exhaust diffuser, as well as the combination of heat sources and exhaust outlet on indoor thermal comfort, vertical temperature difference, contaminant concentration distribution in the breathing zone, quality of inhaled air and energy saving. For the indoor environment, there are many sources of the pollution and some of them are generated by heat sources and human activity while the others come from outdoor surrounding [25, 26]. Generally, most indoor contaminants in an office arise from furniture, work station equipment and by occupants' activities and may contain chemical substances, these locations are very close to the occupants and were investigated by many researchers, while limited or inadequate investigations were performed for the contaminants that were coming from outdoor. Thus, this paper investigates the contaminant effects coming from outside, which are released from sources relatively away from occupied zone. The contaminants were released from two sources, window and door frames, of the same size and at the same time to simulate contaminants coming from outside and entering

the domain from these locations. The concentration distribution of the contaminants in both the occupied zone and inhaled air zone were also evaluated for each case study.

2. Methods

2.1. Case description

The influences of the various locations of the exhaust outlet diffuser and their relation with the heat sources in a room on indoor thermal environment and energy saving were investigated numerically in a typical small office with the dimensions of 4.0 m long, 3.5 m wide, and 2.7 m high. Heat sources in the office included two occupants, two computer cases, two monitors, two ceiling lamps and heat gain from the external wall. The other bounded walls, ceiling and floor were supposed to be adiabatic. The heat emitted from each heat source is listed in Table 1.

Two sources of contaminant were used in this study to simulate contaminants coming from outside and entering the domain through the window and door frame (line sources). A 0.7 μm of particle size with density of 912 kg/m^3 was generated for each case study. This particle size belongs to particles in accumulation mode (0.1-2 μm) such as those found in building dust and smoke. With the DV system, fresh and cool air is normally supplied at or close to the floor level with low velocity. Furthermore, a stratification of temperatures and contaminant concentration is formed in the room and the horizontal temperature profile is uniform except for the region near the DV supply and heat sources. In this study, the supply DV (1.0 m ×0.6 m) inlet was located at the floor level of the side wall and the return opening (1.2 m × 0.2m) was located at the upper boundary of the occupied zone, 1.3 m from the floor level, as recommended by Cheng et al. [18]. The set room temperature in the occupied zone was 24°C. Eighty percent of the supplied air was recirculated from a return opening and the rest of the air was extracted from the exhaust opening at five different locations, as listed in

Table 2. The total supply air flow rate was 94 l/s, which is equal to 9 ACH (air change per hour). The indoor air quality and the occupant productivity can be improved by increasing the ventilation rate [27], hence a high ventilation rate was used in this study. The supply temperature was 19 °C. Fig.1 shows the arrangement of the heat source and contaminant source locations in the simulated room.

Table 1
Cooling load for the simulated office room.

Internal heat sources.	Cooling load (W)
Occupants	80×2
PC_case	50×2
PC_monitor	65×2
Ceiling lamps	60×2
External wall	502
Total	1012
Heat density	72 W/m^2

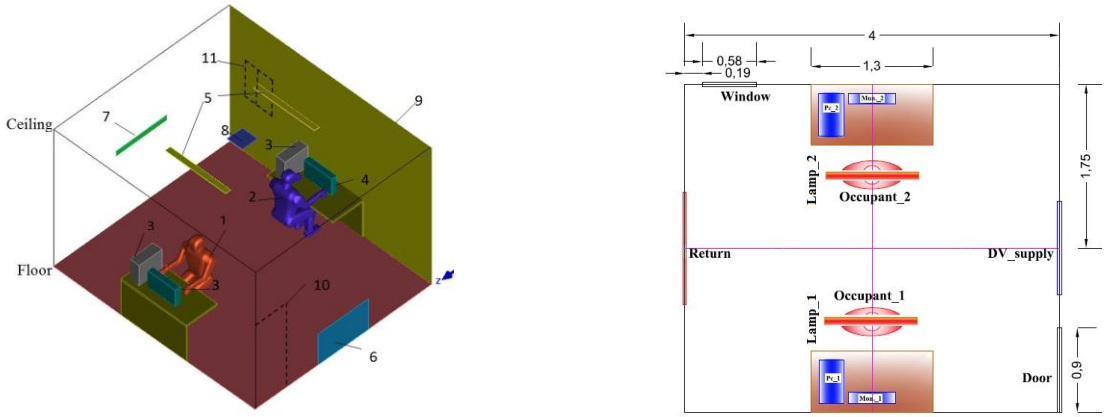

(a) (b)

Fig. 1 (a) Configuration of simulated room; 1- occupant_1; 2 – occupant_2; 3 – PC case; 4- PC monitor;5- lamps; 6- displacement ventilation (DV) inlet; 7- return inlet; 8- exhaust inlet; 9- external wall; 10- contaminant source (line source) at door; 11- contaminant source at window (line source), and (b) the arrangement of the equipment of the simulated office.

Table 2
Case studies description.

Case study	Exhaust location
Case 1	Centre of ceiling between two heat sources (ceiling lamps).
Case 2	Ceiling level, at external wall.
Case 3	Combined with light slots.
Case 4	Ceiling level above (DV) supply opening (slightly away from heat sources).
Case 5	Combined with return opening.

2.2. Computational model

2.2.1 Air flow modelling

For good prediction of indoor air movement and contaminant dispersion, a suitable turbulence model needs to be selected from the various existing models. The two–equation renormalized group RNG $k-\varepsilon$ turbulence model was implemented to predict the turbulence air flow. This model produces an accurate prediction of indoor air flow, temperature and contaminant distribution [28-31]. The RNG $k-\varepsilon$ form, similary to that of the standard $k-\varepsilon$ turbulence model can be expressed as [32]:

$$\frac{\partial(\rho k)}{\partial t}+\frac{\partial(\rho k u_i)}{\partial x_i}=\frac{\partial}{\partial x_j}\left[\left(\mu+\frac{\mu_t}{\sigma_k}\right)\frac{\partial k}{\partial x_j}\right]+P_k+\rho\varepsilon \quad (1)$$

$$\frac{\partial(\rho \varepsilon)}{\partial t}+\frac{\partial(\rho \varepsilon u_i)}{\partial x_i}=\frac{\partial}{\partial x_j}\left[\left(\mu+\frac{\mu_t}{\sigma_\varepsilon}\right)\frac{\partial \varepsilon}{\partial x_j}\right]+C_{1\varepsilon}\frac{\varepsilon}{k}P_k+C_{2\varepsilon}^{*}\rho\frac{\varepsilon^2}{k} \quad (2)$$

where

- $C_{2\varepsilon}^{*}=C_{2\varepsilon}+\left(C_\mu\eta^3(1-\eta/\eta o)\right)/1+\beta\eta^3$ with $\eta=(Sk/\varepsilon)$ and $S=\sqrt{2S_{ij}S_{ij}}$,

The constant values of the RNG $k-\varepsilon$ turbulence model are shown below:

- C_μ =0.0845, σ_k =0.7194, σ_ε =0.7194, $C_{\varepsilon1}$ =1.42, $C_{\varepsilon2}$ =1.68, ηo =4.38 and β =0.012.

For this simulation, the CFD program ANSYS©FLUENT (version R 15.0) was used to solve the Navier-Stokes equations and calculate the Lagrangian trajectories in a 3D computational model of the office. The enhanced wall treatment with reasonable value of y^+ was applied to the near wall cells. Boussinesq assumption was employed to calculate the change in air density due to variations of temperature. The semi-implicit method for pressure-linked equations (SIMPLE) algorithm was chosen for pressure and velocity field coupling, and the second order upwind discretization scheme was chosen to solve all the variables in the simulation cases except pressure which was solved by a staggered scheme named pressure staggering option (PRESTO!). In the present study, the discrete ordinates (DO) model [33] was adopted to simulate the radiation heat transfer emitted from internal heat objects. The details of the numerical methods and boundary conditions are summarized in Table 3.

Table 3
Numerical methods and boundary condition details.

Turbulence model	Renormalized group RNG k − ε turbulence model
Radiation Model	Discrete ordinates (DO) radiation model
Numerical Schemes	For pressure, Staggered third order scheme PRESTO!; for other terms, upwind second order; SIMPLE algorithm
Ceiling, floor, tables and bounded walls	Adiabatic wall
Supply air	Velocity inlet (94 L/s , 19 °C)
Return air	Velocity inlet in negative direction (75.2 L/s)
Exhaust	Pressure –outlet
Occupants	Uniform heat flux 80 W×2
PC_case	Uniform heat flux 50 W ×2
PC_monitor	Uniform heat flux 65 W ×2
Lamps	Uniform heat flux 60 W ×2
External wall	Uniform heat flux 502 W

2.2.2 Discrete phase model

Particle concentration distribution is generally predicted using either the Eulerian-Eulerian or the Eulerian-Lagrangian method for the steady state particle concentration in the

domain [34]. In this study, the Eulerian-Lagrangian model, known as a discrete phase model (DPM), was applied to track the particles through the fluid phase. The Eulerian approach was used to simulate the continuous phase (air flow field), while the Lagrangian approach was used to simulate the discrete phase (airborne particles). The continuous phase was treated as a continuum and solved using the Navier-Stokes equations, while the discrete phase was solved by tracking individual particles through the calculated air flow field. As the particle volume fraction was sufficiently small, the interaction between the two phases was assumed to be one way coupling; i.e. the particles were influenced by the drag and turbulence of airflow field but there was no influence of the particle on the continuous phase [35]. Particle size is classified into three modes: ultrafine (< 0.1μm); accumulation (0.1-2 μm) and coarse (> 2 μm) [36]. In order to simulate the contaminant distribution coming from outside and entering the domain, this study employed the accumulation mode to predict the contaminant concentration distribution in the breathing zone and the quality of inhaled air for each case.

2.2.2.1 Particles tracking equations

The Lagrangian approach is used to calculate the individual trajectories of each particle by solving the momentum equation. By equating the particle inertia to the external forces, the momentum equation can be expressed as:

$$\frac{d\vec{u}_p}{dt} = F_D\left(\vec{u} - \vec{u}_p\right) + \frac{\vec{g}(\rho_p - \rho)}{\rho_p} + \vec{F}_a \quad (3)$$

where the inertial force per unit mass ($m\,s^{-2}$) is represented in the left-hand side of Eq. (3), and the drag forces per unit mass are expressed in the first term of the right hand side. The gravitational and buoyancy forces are represented in the second term; $\vec{F}_a$ is used to add the additional forces (per unit mass) which may have an impact on particle motion. In the present work, the drag force is the most important force acting on the particles and it follows the Stokes drag law:

$$\vec{F}_{drag} = F_D(\vec{u} - \vec{u}_p) = \frac{18\mu}{\rho_p d_p^2 C_c}(\vec{u} - \vec{u}_p) \quad (4)$$

where C_c is the Cunningham correction factor which is calculated from:

$$C_c = 1 + \frac{2\lambda}{d_p}\left(1.257 + 0.4e^{-(1.1d_p/2\lambda)}\right) \quad (5)$$

In this study, the Basset history, pressure gradient and virtual mass were negligible or had no influence compared to the drag force. For ventilated rooms, the Brownian motion, thermophoretic and Saffman's lift are two orders of magnitude smaller than the Stokes drag force and occasionally these forces become compatible with Stokesian drag force when fine size particles are used in fluid flow field [37]. The Brownian motion and Saffman lift forces may become considerable and influence the particle motion, especially in the turbulent boundary layer near the walls [38]. In addition, these forces may play a significant role in the deposition process [39-41], therefore, they were taken into consideration in this study. The final form of trajectory equation can be expressed as:

$$\frac{d\vec{u}_p}{dt} = F_D(\vec{u} - \vec{u}_p) + \frac{\vec{g}(\rho_p - \rho)}{\rho_p} + \vec{F}_b + \vec{F}_{thermal} + \vec{F}_s \quad (6)$$

In turbulent flow, the particles path is significantly affected by local turbulence intensities. In order to simulate the stochastic velocity fluctuations in airflow, the discrete random walk (DRW) approach was used in this study [42]. The instantaneous velocity is represented by time-averaged flow field velocity $\bar{u}_i$ and fluctuating velocity u_i'. The final form of the fluctuating velocity components become:

$$u_i' = \xi_i\sqrt{\bar{u}_i'^2} = \xi_i\sqrt{2k/3} \quad (7)$$

As a result of the assumption of the one way coupling between two phases, the air flow field is solved first, and subsequently the particles are injected [43]. As mentioned previously, the air flow equations and Lagrangian trajectories were calculated using ANSYS Fluent software. However, the Lagrangian approach does not directly calculate the

concentration of the particles in the domain. Therefore, this study used a user-define function (UDF) to calculate the concentration distribution of the particles from the trajectories. In order to calculate the particles concentration distribution in fluid flow field, it is important to correlate the concentration with the trajectories for each computational cell in the domain. This can be achieved using particle source in-cell (PSI-C) scheme based on following equation:

$$C = \frac{\dot{m} \sum_{i=1}^{n} dt(i,j)}{V_j} \quad (8)$$

The accuracy and the simulation stability of the Lagrangian model was investigated by Zhang and Chen [34] and, based on their studies, the calculations of concentration are statically stable when a sufficient number of trajectories are tracked in the domain. Therefore, in the present study, adequate numbers of particle trajectory have been tracked.

2.2.2.2 Boundary conditions

Particles escape and their trajectories terminate when they reach the inlets and exhaust outlets in the domain. When particles reach solid objects, they may attach to or rebound from the surface of these objects. In a ventilated room, particles are most likely to attach to the rigid body surface because they do not have enough energy to rebound to overcome adhesion [44]. When the mesh at the walls is not fine enough, the results will over predict the viscous sub-layer kinetic energy and the fluctuating velocity will increase in these regions which will increase the collision of particles with the walls. In this study, the inflation boundary layer was used near the walls with enough mesh refinement. Therefore, the particle collisions in these regions (near walls) were predicted accurately and the trap boundary condition was applied.

3. Validation of the CFD algorithm

3.1. Validation of fluid flow

An experimental study on air velocity distribution and temperature distribution in a room environment was performed by Xu et al. [45]. This work was chosen to validate the accuracy of the current turbulence model in prediction of the indoor thermal environment. Fig.2 a shows the schematic diagram for the experimental chamber. The simulation was performed in a typical small room with the dimensions of 6.0 m long, 3.9 m wide, and 2.35 m high with two heat sources included one occupant (76 W) seat in front of table and one computer (40 W) located on the table (see Fig.2 a). Two poles, pole 1 and 4, were used in this validation to predict the temperature and velocity distribution (see Fig. 2 b). The supply and exhaust diffuser dimensions were (0.4 m ×0.15 m) and (0.34 ×0.14 m) respectively. The supply air flow rate was 43 m^3/h which is equal to 0.79 ACH (air change per hour). The supply temperature was 19 °C. Different temperatures value was used for the bounded walls, ceiling and floor. Fig. 2 c and d show a good agreement between the measured and simulated results. All the details can be found in Xu et al.'s publication [45].

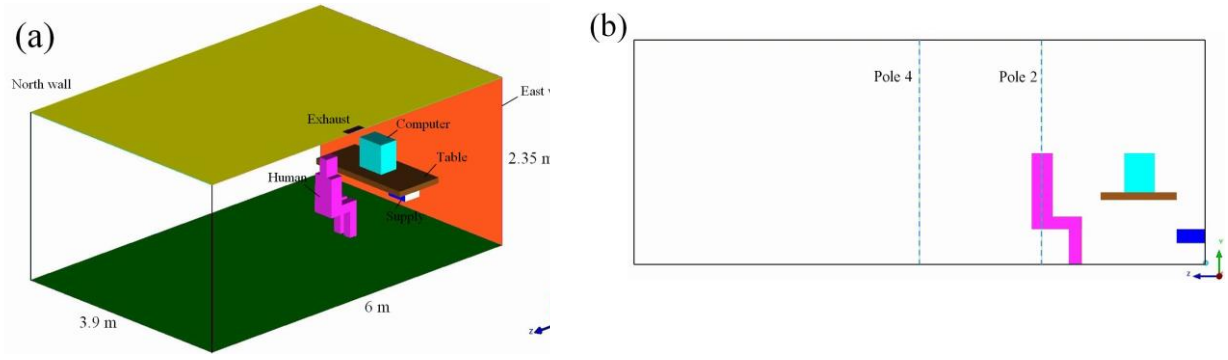

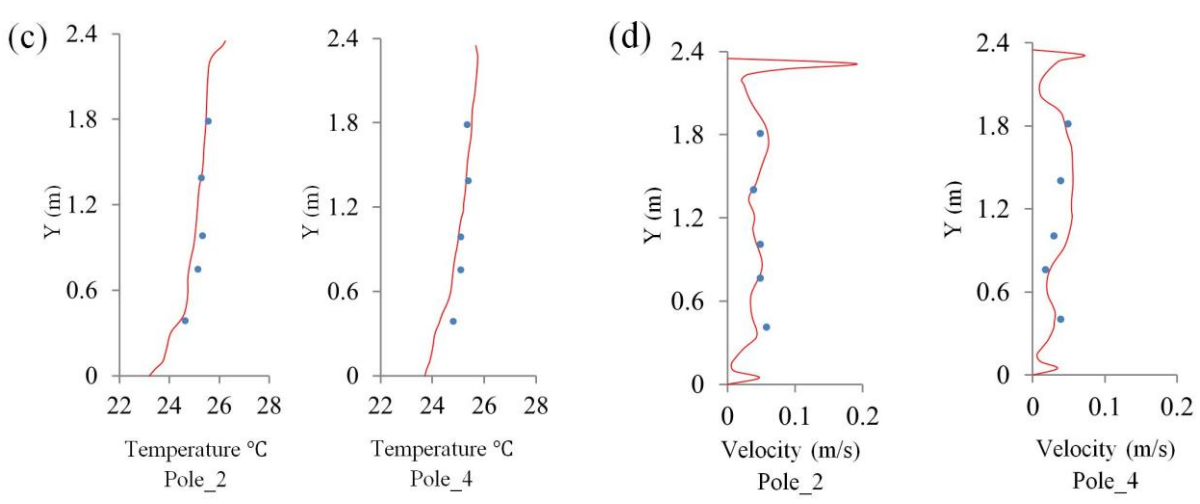

Fig. 2. (a) Schematic diagram of the validation room model [45]; (b) poles 1 and 2 location; (c) and (d) comparison between the simulated and experimental temperature and velocity profiles at two vertical poles; (c) temperature distribution and (d) velocity distribution; (circle symbol: experimental results [45] ; solid line: simulated results by authors).

3.2. Particle transport validation

To validate the Lagrangian particle-tracking model, the experimental results of Chen et al. [46] are used to show the accuracy of this model. As shown in Fig. 3, the dimensions of the room were 0.8 m × 0.4 m × 0.4 m. The inlet and the outlet had the same dimensions (0.04 m ×0.04 m) and were located at the centre of the test chamber. The supply velocity was 0.225 m/sec and the particle diameter was 10 μ m with 1400 density. Particle concentration was normalised by the concentration of inlet. Fig.4 illustrates the comparison between the normalised concentration and the experimental data at three different locations. A reasonable agreement between the predicted and experimental results can be seen from these graphs.

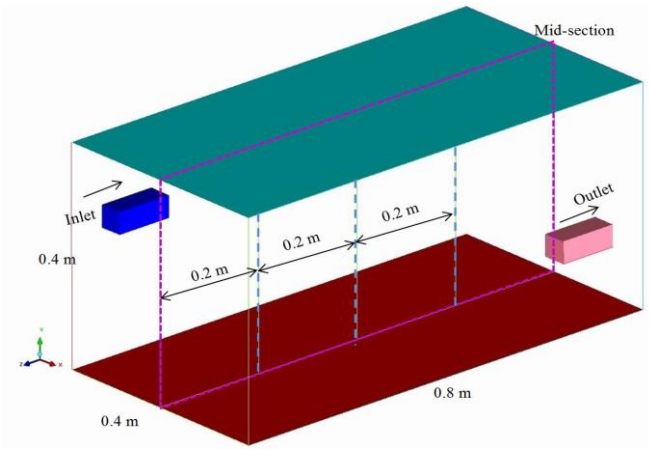

Fig. 3. Schematic diagram of ventilated chamber of the validation case of Lagrangian particle-tracking [46].

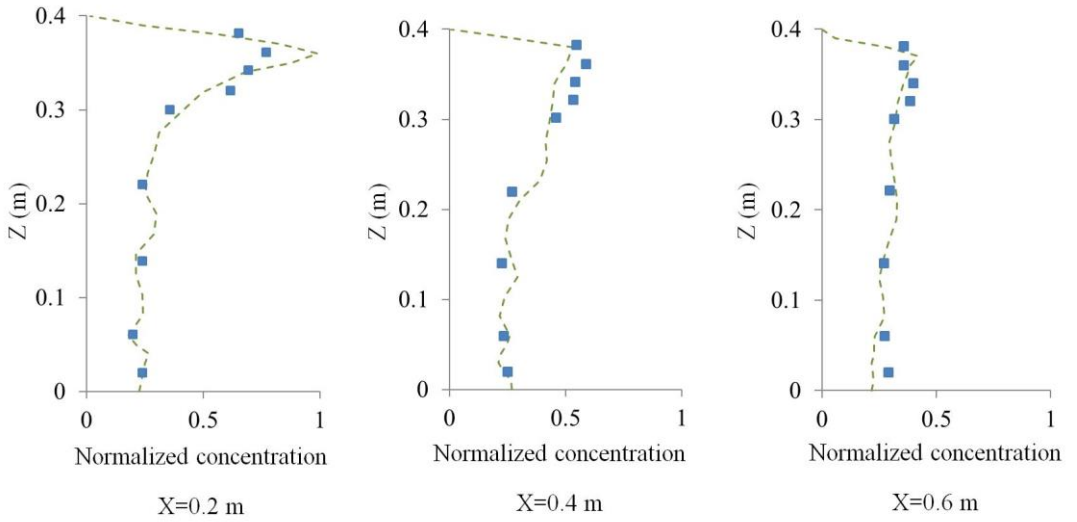

Fig. 4. Comparison between the normalized particle concentration and experimental data [46] at different locations x=0.2, 0.4 and 0.6 (square symbols: experimental data [46]; dashed line: normalized particle concentration by authors).

3.3 Grid independence

As a result of the room and equipment complexity, ANSYS ICEM CFD software was used in this study to generate a tetrahedral unstructured mesh with inflation boundary layer around the occupants and different element size. The grid around the occupants and others heat objects were fine enough to capture the thermal environment behaviour and solving the boundary layer. The surface grid was generated for the occupants, computers and monitors with 1 cm of element size, and 5 mm for the ceiling lamps. The mesh was clustered in regions

that have high gradients of temperature and velocity such as bounded walls, ceiling floor and table. For the mesh test, In order to control the total number of cells, only the element size in the domain was changed without changing the surface grid size for the internal heat sources and walls. In order to resolve the boundary layer around the occupants, an inflation boundary layer was generated with the first layer thickness of 1.5 mm, 4 layers with 1.2 of growth rate (see Fig.5). A satisfy the requirement of y^+ values, ranged between $0.7 \leq y^+ \leq 4.5$, was achieved. Mesh independence test plays a significant role in CFD simulation regarding results accuracy and prediction cost. In the current study, the proper size of grid was selected by comparing the simulation results for three different sizes of grid as listed in Table 4. By comparing the simulation results for the temperature and velocity distribution for each grid size, there is no significant change in temperature and velocity distribution with increasing the grid cells from mesh_2 to mesh_3, Therefore, mesh 2 was selected to be the proper grid size for the rest of the simulation.

Table 4
Mesh independent test.

Mesh types.	Cells number
Mesh_1	865,235
Mesh_2	1,705,689
Mesh_3	2,415,523

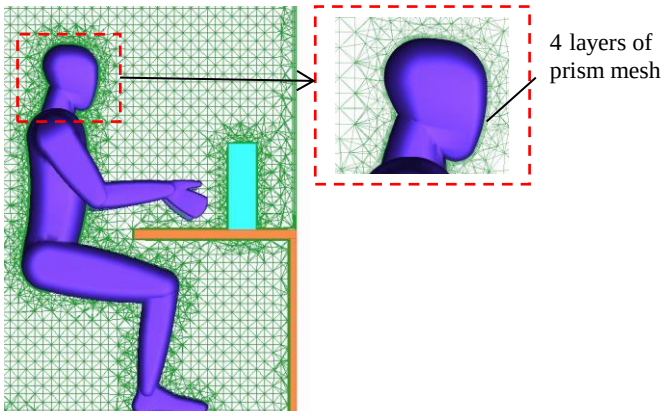

Fig. 5. Inflation boundary layer around the human body.

4. Results and discussion

4.1. Thermal comfort evaluation

The indoor thermal comfort indices are assessed using Fanger's comfort equations [47]. In this model, the thermal balance for the whole human body is represented by two indices PMV and PPD. For the indoor thermal comfort requirement, appropriate PMV and PDD values are in the range -0.5< PMV< 0.5 and PPD < 10 percent respectively.

The PMV and PPD indices were used to evaluate the thermal comfort condition in each case study. Fig. 6 presents the PMV and PPD results for both occupants for each case. The PMV and PPD indices for each occupant were approximately the same with only a slight difference between them; this was due to the fact that the thermal environment around the occupants in the area near the external wall was influenced by the heat flux of the external wall which subsequently affected the thermal comfort of the occupants in this region. Similar findings were reported by Horikiri et al. [48]. Small PPD and PMV values are highly recommended for indoor human thermal comfort requirements [49]. The PPD and PMV indices values were in the acceptance range (i.e. below 10% for PPD and between 0.5 to -0.5 for PMV) for four of the five cases, cases 1, 2, 3 and 4 (see Fig. 6). For further explanation, Fig. 7 (a-e) and Fig. 8 (a-e) show the temperature and velocity distribution for each case study at different section planes. These figures show that by locating the exhaust diffuser at ceiling level, near or combined with heat sources, the room air temperature distribution and velocity improved and tended to provide uniform distribution in most of the room's domains which caused a comfortable thermal environment around the occupants. On the other hand, when the exhaust diffuser was combined with the return outlet in one unit away from the room's heat sources, as in case 5, the occupants became thermally unsatisfied and the thermal environment was uncomfortable in most of the room's domains compared with the other cases, this was due to the large amount of relatively fresh air coming from the supply

diffuser extracted directly from the combined unit diffuser in the occupied zone before mixing with the rest of the air in the room. In addition, the thermal plumes generated from the room's heat sources led to an increase in the temperature in the upper part of the room and the supply conditioned air do not effectively mixed with warm air in the upper part of the room. All these factors created a non-homogeneous distribution of temperature; velocity and uncomfortable environment around the occupants as shown in Fig.7 and 8 (e). There was no influence of velocity field on the PPD and PMV calculations, as most of the velocity measured at the calculation points was very small (below 0.05 m/sec)

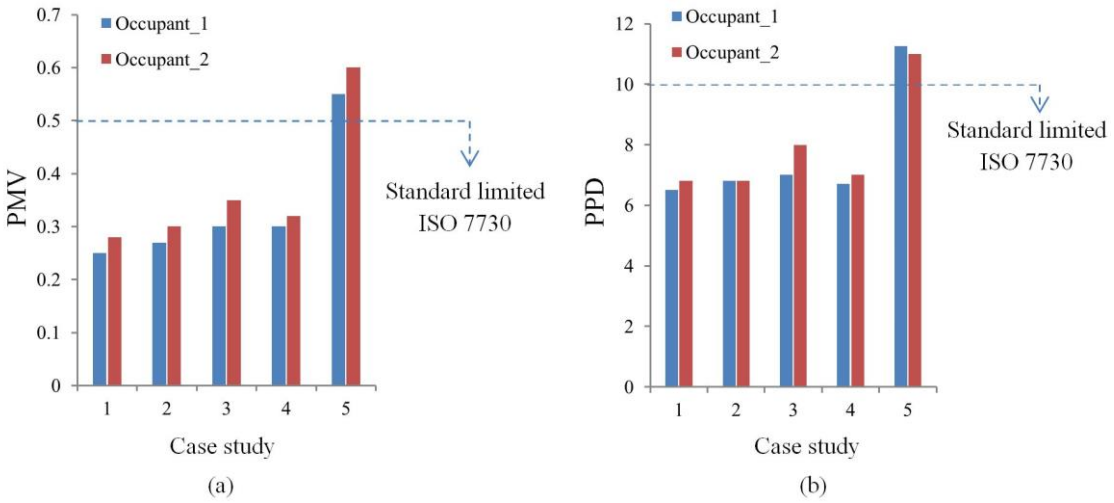

Fig.6. Indoor thermal comfort in each case study for both occupants; (a) PMV index; (b) PPD index.

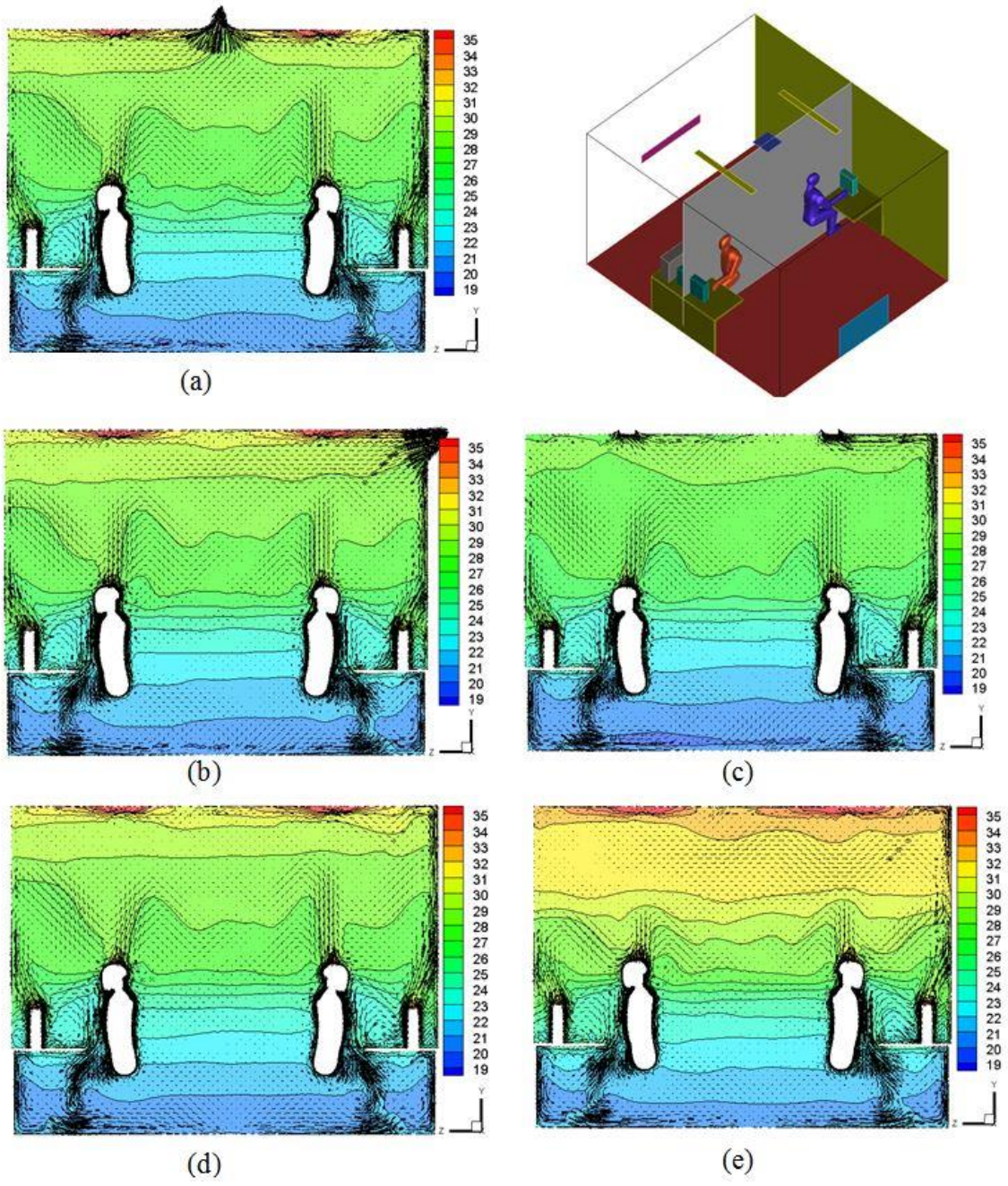

Fig. 7. Temperature (°C) and velocity distribution (m/s) at the central plane x=2 m for all case study: (a) case 1; (b) case 2; (c) case 3; (d) case 4; (e) case 5.

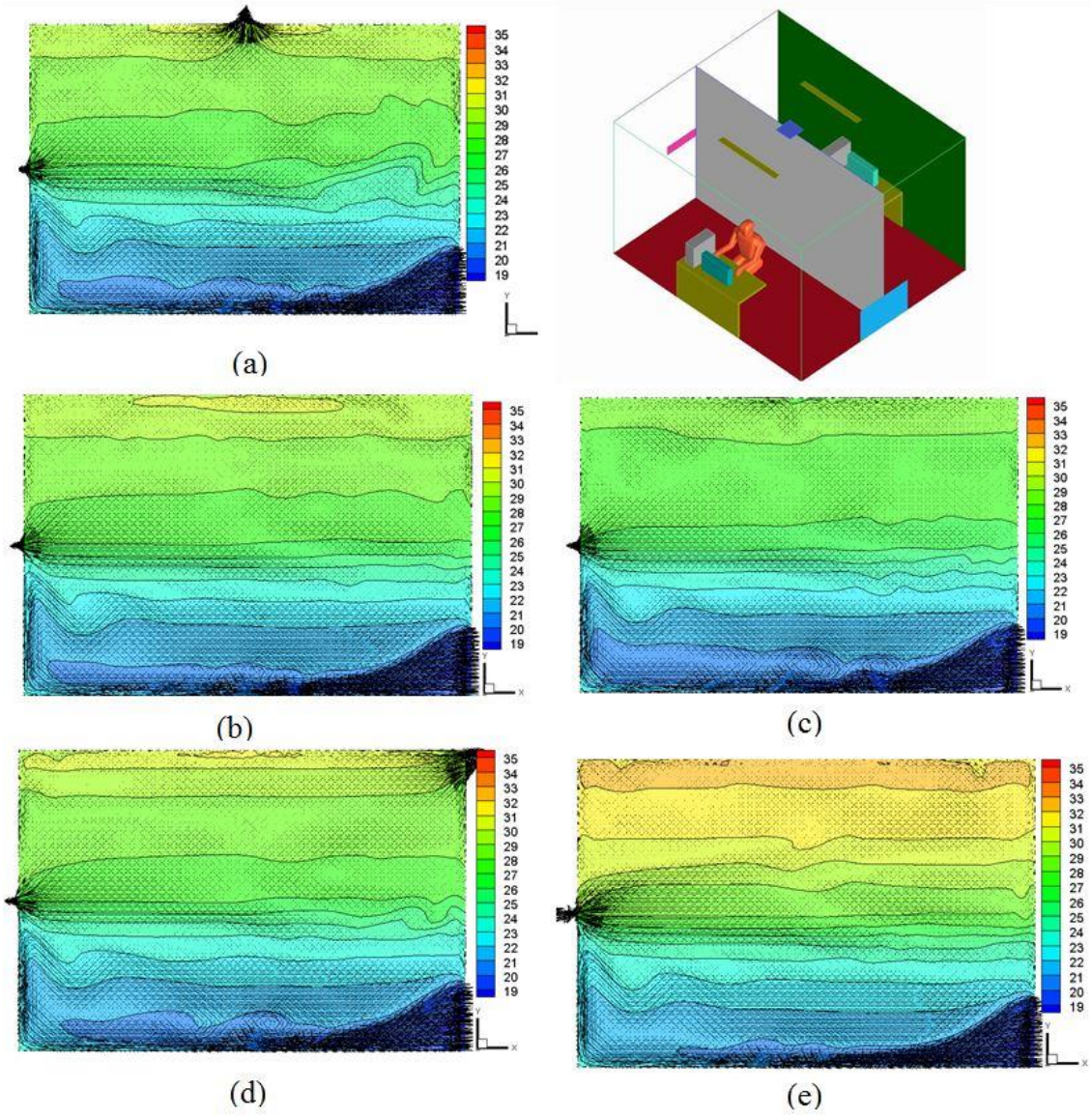

Fig. 8. Temperature (℃) and velocity distribution (m/s) at the central plane, y =1.75 m, for all case study; (a) case 1; (b) case 2; (c) case 3; (d) case 4 and (d) case 5.

4.2. Local thermal discomfort

The vertical temperature difference is one of the main factors in assessing indoor thermal comfort in a stratified air distribution system STARD. According to the ISO7730 [49], the temperature difference between the head and foot level ($\Delta T_{head-foot}$) should not exceed 3 ℃. The local thermal discomfort index was used to evaluate the vertical temperature difference in the region around the occupants. Four positions (points I, II, III and IV), two points at each occupant, were used in this study to assess the thermal discomfort in each case (see Fig. 9 a). As shown in Table 5, the ($\Delta T_{head-foot}$) values for cases 1, 2, 3 and 4 were in the accepted range for most locations and slightly higher at point I; the reason is that the location of this point was close to the supply inlet diffuser. Similar findings were revealed by Lian and Wang [50].

Table 5
Temperature gradient between the head and foot levels for occupants (°C).

Case study	Occupant_1		Occupant_2	
	Point I	Point II	Point III	Point IV
Case_1	3.5	3.0	3.0	3.0
Case_2	3.0	3.0	2.7	3.0
Case_3	3.0	2.8	2.7	2.9
Case_4	3.2	3.0	2.9	3.1
Case_5	3.7	3.6	3.5	3.6

For a detailed explanation of temperature distribution in a vertical direction, Fig.9 (b, c, d and e) presents the vertical temperature difference at different positions, poles I, II, III and IV, in each case study. In cases 2 and 3, when the exhaust outlets were combined with the heat sources (lamps and external wall) the ($\Delta T_{head-foot}$) values were in the acceptance range at all points. The reason is that most of the heat flux emitted from these sources was extracted directly from the exhaust outlet diffuser before mixing with the air in the occupied zone which led to the temperature gradient between the upper and lower parts being reduced

as shown Fig. 7 and 8 (a, b and c), while for case 5, when the exhaust was combined with the return outlet, the temperature gradient was out of range for all the monitoring points. This is because part of the supply of fresh air was directly extracted from the combined outlet (return with exhaust) before mixing with the warm air in the occupied area. The temperature gradient between the upper and lower parts of the room was relatively high compared to the other case study (see Figs. 7 and 8 e) because a small amount of cold and fresh air was induced by the thermal plumes and reached the upper part of the room [51], causing an increase in the room air temperature in this area.

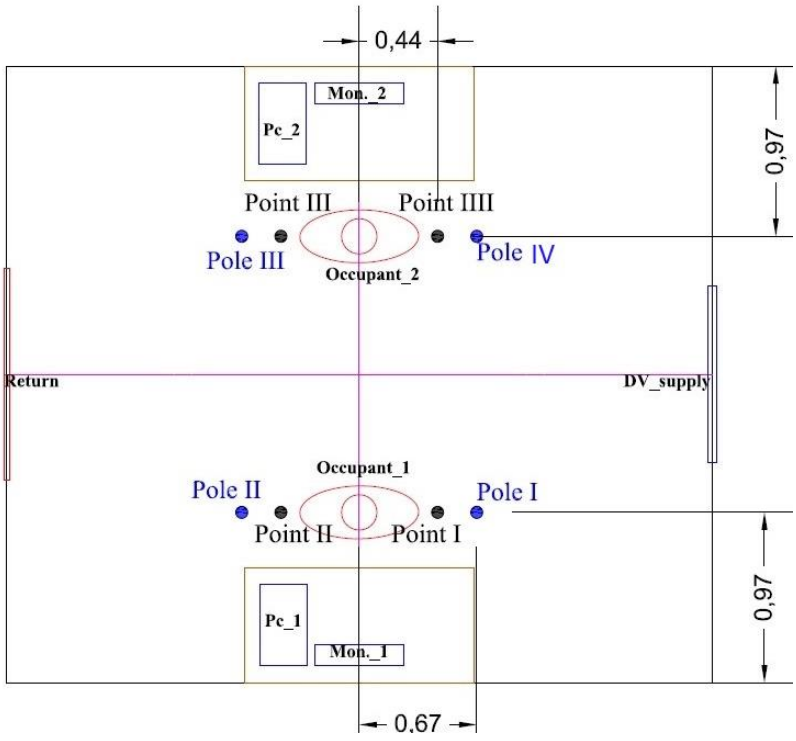

(a)

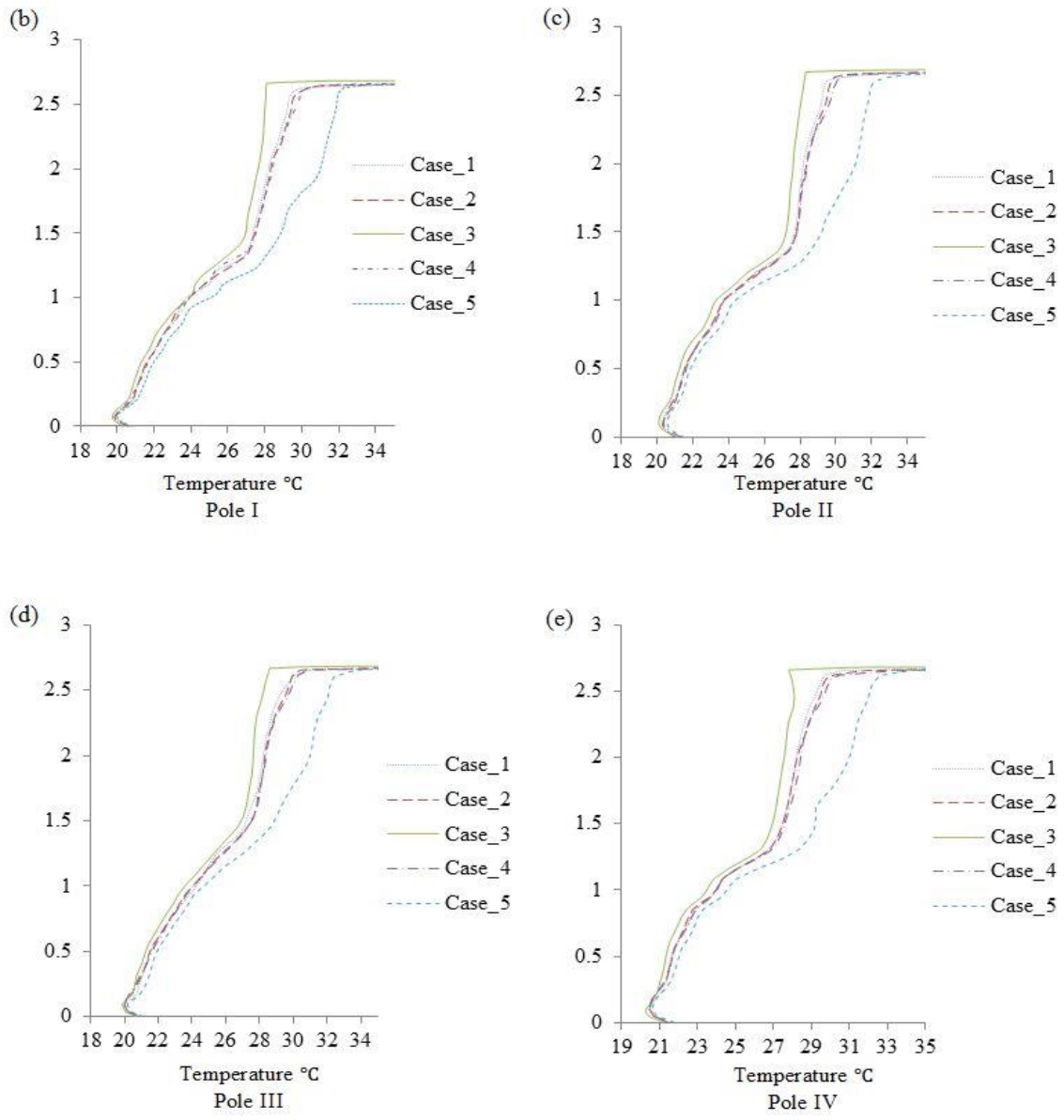

Fig. 9.Temperature distribution in vertical direction for different cases (a) monitoring points and pole locations ; (b),(c),(d) and(e) are the vertical temperature distribution in pole 1,2,3and 4 respectively.

4.3. Energy saving

In the stratified air distribution (STRAD) system, only the area in the occupied zone is required to be thermally comfortable which increases the potential to reduce energy consumption. In this system the fresh air moves up by thermal plumes towards the ceiling by natural convection where it warms up by contacting internal room heat sources. Stratification

of temperatures is formed in the room and the horizontal temperature profile is uniform except for the region near the supply diffuser and heat sources. The energy savings were evaluated for each case study to show the impact of exhaust location on energy saving. Based on CFD simulation results, Cheng et al. [18] developed a method to calculate the reduction in cooling coil load in a room using the STRAD system. For the same set room temperature (T_{set}), the calculation of cooling coil load in the STRAD system is different from that in the mixing ventilation (MV) system:

$$Q_{coil-STRAD} = Q_{coil-MV} - c_p \times \dot{m}_e \times (T_e - T_{set}) \quad (9)$$

$$Q_{coil-MV} = Q_{space} + Q_{vent} \quad (10)$$

where $Q_{coil-STRAD}$ and $Q_{coil-MV}$ represent the cooling coil load for the STRAD system and MV system respectively; Q_{space} and Q_{vent} are the cooling coil load of space and ventilation load respectively and T_{set} is the room set temperature which was 24℃ for all case studies. The term $c_p \times \dot{m}_e \times (T_e - T_{set})$ refers to the amount of cooling coil load reduction which is widely used to evaluate the energy saving in the STRAD system [11, 18, 52, 53] . This term was used in the present work to calculate the amount of energy saving for each case.

Table 6 illustrates that the reduction of cooling coil load was proportional with exhaust temperature in each case. In cases 1, 2 and 3 the energy efficiency was the best when the exhaust outlet diffuser was combined or located near the heat sources (lamps and external wall), This is because the direct extraction of the heat flux from these heat sources contributed to an increase in the exhaust temperature, consequently improving the potential for energy saving. In addition, due to the reduction of air temperature in all domains of the room (see Fig 8), the less warm air in the occupant boundary entered the return grill which contributed to a reduction in the coil load. In contrast, in case 5 when the exhaust outlet was

located away from room heat sources and combined with the return outlet, the relatively high warm air (see Fig. 7 and 8 e) was recirculated and entered the return grill, causing increased energy consumption. Thus, energy saving was significantly increased to 25.0%, 13.8% and 12.65 % in cases 3, 1 and 2 respectively. From these results we can conclude that the amount of energy saving depends on the distance between the exhaust diffuser and the heat sources as well as the combination of heat sources with exhaust opening, i.e. extra energy saving can be achieved by locating the exhaust diffuser close to the heat object. In order to select the appropriate locations for exhaust diffusers, other factors such as the thermal comfort indices, vertical temperature difference and contaminant concentration distribution should be considered carefully.

Table 6
Energy saving for cooling coil.

Case study	T_e (°C).	T_r (°C).	$\Delta Q_{coil} = C_p \times \dot{m_e} \times (T_e - T_{set})$ (W).	$\Delta Q_{coil}/\Delta Q_{space}$ (%)
Case_1	30.0	26.6	139.6	13.8
Case_2	29.5	26.7	128.0	12.65
Case_3	34.0	26.0	250.0	25.0
Case_4	29.3	26.7	123.0	12.18
Case_5	27.6	27.6	85.0	8.4

4.4. The quality of indoor air evaluation

The quality of the indoor air plays a significant role in the evaluation of the indoor air distribution system performance, particularly in terms of the distribution and concentration of contaminants. The most important factors that affect particle concentration distribution in a room are the location of exhaust diffusers and contaminant sources. In the current work, the contaminant sources were located at the door and window frames to simulate contaminants coming from outside and entering the domain from these frames with the same particle diameter as shown in Fig. 1. The quality of the occupants' inhaled air (see Fig. 10) and the air

quality in the breathing zone, 1.3 m from floor level, were used to evaluate the air quality for each case. The contaminant concentration normalisation is defined as follows:

$$C_n = \frac{C_p}{C_e} \tag{11}$$

Figs. 11 a and b compare the normalised particle concentration for each case study in the inhaled and breathing zones respectively. It is clear that the particle concentration for occupant 1 was larger than the concentration for occupant 2 in all cases except case 3. The reason for this is that the position of occupant 1 was very close to the door contaminant sources. This is consistent with findings reported by Licina et al. [25]. In addition, occupant 2 was located near the external wall, where the contaminant transport was greatly influenced by the convective heat flux that contributed to bringing a large amount of contaminants from the occupant zone towards the extract outlet at ceiling level which consequently improved the inhaled air for occupant 2. Furthermore, in cases 1, 2, 3 and 4 the air in the inhaled area and the breathing zone showed better quality for both occupants compared with case 5 (see Fig. 11 a and b). This is because the contaminants transported by the thermal heat plumes from heat sources in the lower part of the room were extracted at ceiling level which consequently reduced the contaminant concentration at both the inhaled air and the breathing levels. In addition, the convective heat from heat sources was significantly affected by the temperature field [54]. On the other hand, for case 5, due to there being no extract opening at the ceiling level, the contaminants in the upper part were still in recirculation and their increased concentration caused a significant increase in all the room's domains, including inhaled air and breathing level. The best air quality for the inhaled zone and breathing zone were achieved in case 3, as the combination of the exhaust and lamp extracted a large amount of contaminants which led to a reduction in the contaminant concentration in both the inhaled and the breathing zones compared with the other case studies.

From these results it is clear that satisfactory air quality can be achieved by locating the exhaust close to the room's heat sources. Similar findings were revealed by Serrano-Arellano et al. [55]. This is because the room's contaminants are mostly carried by thermal plumes of heat source and extracted directly from the exhaust outlet which contributes to reducing the contaminant concentration in the room's domains.

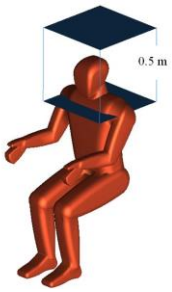

Fig. 10. inhaled area around the occupants 0.5m cubic (microenvironment).

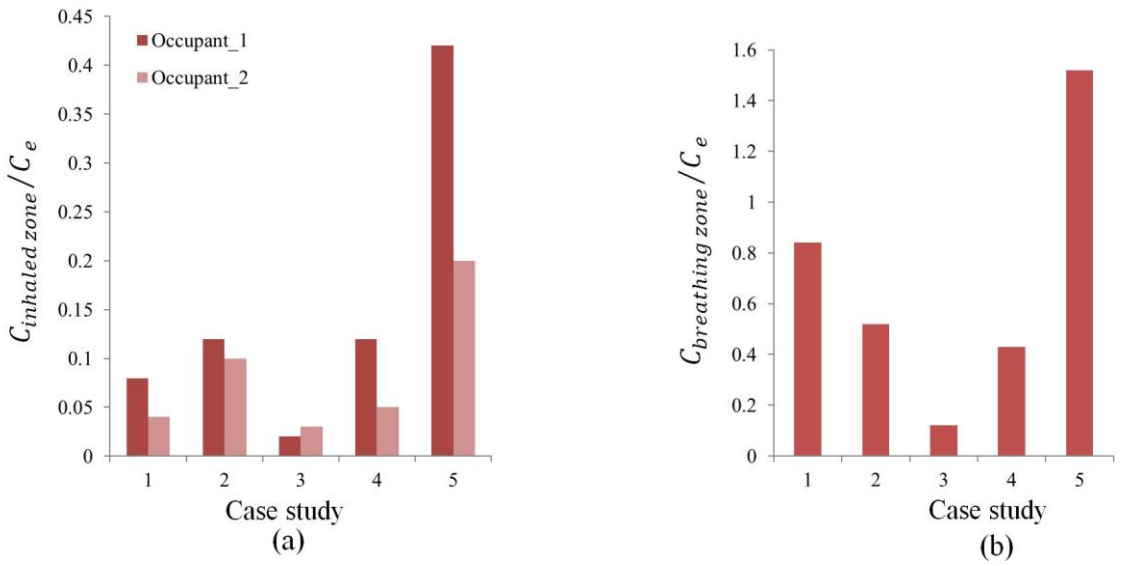

Fig. 11. Comparison of the particle concentration for each case study; (a) for inhaled area for each occupant; (b) for breathing level.

5. Conclusion

In this study, the effects of the locations of the exhaust air vent on the indoor thermal comfort, vertical temperature difference, contaminant concentration in the occupied zone,

quality of inhaled air and energy saving in an office were investigated. The results of this study concluded as follows:

- A significant improvement on energy saving and quality of inhaled air was made when the exhaust was combined with the room heat sources, such as in case 1 when the exhaust is located between two heat sources, and in cases 2 and 3 when the exhaust is combined with the external walls and room's ceiling lamps, respectively.
- In case 3, a 25.0 % of energy saving was achieved by combining the exhaust diffuser with room's ceiling lamps. Furthermore, locating the exhaust diffuser near the heat sources, cases 1 and 2, also reduced the cooling coil load by 13.8 % and 12.65 % respectively. While in case 5, when the exhaust and return outlets were combined in one unit at the occupied boundary area, the risk of thermal discomfort and poor air quality in the occupied zone, as well as energy consumption, was clearly increased.
- The enhancement of the IAQ in the breathing zone and the quality of the inhaled air were most significant when the exhaust was separated from the return opening, and combined with the heat sources, as shown in case 3.
- Overall, better indoor thermal environment in terms of thermal comfort, temperature distribution, quality of indoor air, inhaled air and energy saving was achieved by combining the indoor heat sources with the exhaust outlet vent at the ceiling level.

6. Acknowledgements

The authors would like to thank the Ministry of Higher Education and Scientific Research of Iraq for the financial support of the project.

References

[1] He G, Yang X, Srebric J. Removal of contaminants released from room surfaces by displacement and mixing ventilation: modeling and validation. Indoor air. 2005;15:367-80.

[2] Budaiwi I, Abdou A. HVAC system operational strategies for reduced energy consumption in buildings with intermittent occupancy: the case of mosques. Energy Conversion and Management. 2013;73:37-50.

[3] Li A, Qin E, Xin B, Wang G, Wang J. Experimental analysis on the air distribution of powerhouse of Hohhot hydropower station with 2D-PIV. Energy Conversion and Management. 2010;51:33-41.

[4] Salvalai G, Pfafferott J, Sesana MM. Assessing energy and thermal comfort of different low-energy cooling concepts for non-residential buildings. Energy Conversion and Management. 2013;76:332-41.

[5] Wong L, Mui K. An energy performance assessment for indoor environmental quality (IEQ) acceptance in air-conditioned offices. Energy Conversion and Management. 2009;50:1362-7.

[6] Kharseh M, Altorkmany L, Al-Khawaj M, Hassani F. Warming impact on energy use of HVAC system in buildings of different thermal qualities and in different climates. Energy Conversion and Management. 2014;81:106-11.

[7] Chu C-M, Jong T-L. Enthalpy estimation for thermal comfort and energy saving in air conditioning system. Energy Conversion and Management. 2008;49:1620-8.

[8] Kanaan M, Ghaddar N, Ghali K, Araj G. New airborne pathogen transport model for upper-room UVGI spaces conditioned by chilled ceiling and mixed displacement ventilation: Enhancing air quality and energy performance. Energy Conversion and Management. 2014;85:50-61.

[9] Gao C, Lee W, Chen H. Locating room air-conditioners at floor level for energy saving in residential buildings. Energy Conversion and Management. 2009;50.

[10] Awad A, Calay R, Badran O, Holdo A. An experimental study of stratified flow in enclosures. Applied Thermal Engineering. 2008;28:2150-8.

[11] Cheng Y, Niu J, Du Z, Lei Y. Investigation on the thermal comfort and energy efficiency of stratified air distribution systems. Energy for Sustainable Development. 2015;28:1-9.

[12] Bagheri H, Gorton R. Performance characteristics of a system designed for stratified cooling operating during the heating season. ASHRAE Trans;(United States). 1987;93.

[13] Filler M. Best practices for underfloor air systems. ASHRAE journal. 2004;46:39-46.

[14] Hongtao X, Naiping G, Jianlei N. A method to generate effective cooling load factors for stratified air distribution systems using a floor-level air supply. HVAC&R Research. 2009;15:915-30.

[15] Rim D, Novoselac A. Transport of particulate and gaseous pollutants in the vicinity of a human body. Building and Environment. 2009;44:1840-9.

[16] Deng Q-H, Zhou J, Mei C, Shen Y-M. Fluid, heat and contaminant transport structures of laminar double-diffusive mixed convection in a two-dimensional ventilated enclosure. International Journal of Heat and Mass Transfer. 2004;47:5257-69.

[17] Park H-J, Holland D. The effect of location of a convective heat source on displacement ventilation: CFD study. Building and environment. 2001;36:883-9.

[18] Cheng Y, Niu J, Liu X, Gao N. Experimental and numerical investigations on stratified air distribution systems with special configuration: Thermal comfort and energy saving. Energy and Buildings. 2013;64:154-61.

[19] Ahmed A, Gao S. Thermal Comfort and Energy Saving Evaluation of a Combined System in an Office Room Using Displacement Ventilation. World Academy of Science, Engineering and Technology, International Journal of Mechanical, Aerospace, Industrial, Mechatronic and Manufacturing Engineering. 2015;9:1078-83.

[20] Thool SB, Sinha SL. Numerical Simulation and Comparison of Two Conventional Ventilation Systems of Operating Room in the View of Contamination Control. International Journal of Computer Applications. 2014;85.

[21] Khan J, Feigley C, Lee E, Ahmed M, Tamanna S. Effects of inlet and exhaust locations and emitted gas density on indoor air contaminant concentrations. Building and Environment. 2006;41:851-63.

[22] Kuo J-Y, Chung K-C. The effect of diffuser's location on thermal comfort analysis with different air distribution strategies. Journal of Building Physics. 1999;22:208-29.

[23] Lin Z, Chow T, Tsang C, Fong K, Chan L. CFD study on effect of the air supply location on the performance of the displacement ventilation system. Building and environment. 2005;40:1051-67.

[24] Zhang T, Chen QY. Novel air distribution systems for commercial aircraft cabins. Building and Environment. 2007;42:1675-84.

[25] Licina D, Melikov A, Pantelic J, Sekhar C, Tham KW. Human convection flow in spaces with and without ventilation: personal exposure to floor-released particles and cough-released droplets. Indoor air. 2015.

[26] Matson U. Indoor and outdoor concentrations of ultrafine particles in some Scandinavian rural and urban areas. Science of the Total Environment. 2005;343:169-76.

[27] Wargocki P, Wyon DP, Sundell J, Clausen G, Fanger P. The effects of outdoor air supply rate in an office on perceived air quality, sick building syndrome (SBS) symptoms and productivity. Indoor air. 2000;10:222-36.

[28] Horikiri K, Yao Y, Yao J. Numerical study of unsteady airflow phenomena in a ventilated room. ICHMT DIGITAL LIBRARY ONLINE. 2012.

[29] Horikiri K, Yao Y, Yao J. Modelling conjugate flow and heat transfer in a ventilated room for indoor thermal comfort assessment. Building and Environment. 2014;77:135-47.

[30] Srebric J, Chen Q. Simplified numerical models for complex air supply diffusers. HVAC&R Research. 2002;8:277-94.

[31] Yuan X, Chen Q, Glicksman LR, Hu Y, Yang X. Measurements and computations of room airflow with displacement ventilation. Ashrae Transactions. 1999;105:340.

[32] Yakhot V, Orszag S, Thangam S, Gatski T, Speziale C. Development of turbulence models for shear flows by a double expansion technique. Physics of Fluids A: Fluid Dynamics (1989-1993). 1992;4:1510-20.

[33] Chandrasekhar S. Radiative heat transfer1960.

[34] Zhang Z, Chen Q. Comparison of the Eulerian and Lagrangian methods for predicting particle transport in enclosed spaces. Atmospheric Environment. 2007;41:5236-48.

[35] Fluent A. Fluent theory guide. Ansys Inc. 2012.

[36] Nazaroff WW. Indoor particle dynamics. Indoor air. 2004;14:175-83.

[37] Zhao B, Zhang Y, Li X, Yang X, Huang D. Comparison of indoor aerosol particle concentration and deposition in different ventilated rooms by numerical method. Building and Environment. 2004;39:1-8.

[38] Li A, Ahmadi G. Dispersion and deposition of spherical particles from point sources in a turbulent channel flow. Aerosol Science and Technology. 1992;16:209-26.

[39] McLaughlin JB. Aerosol particle deposition in numerically simulated channel flow. Physics of Fluids A: Fluid Dynamics (1989-1993). 1989;1:1211-24.

[40] Nazaroff WW, Cass GR. Mathematical modeling of indoor aerosol dynamics. Environmental Science & Technology. 1989;23:157-66.

[41] Rizk M, Elghobashi S. The motion of a spherical particle suspended in a turbulent flow near a plane wall. Physics of Fluids (1958-1988). 1985;28:806-17.

[42] Wang M, Lin C-H, Chen Q. Advanced turbulence models for predicting particle transport in enclosed environments. Building and Environment. 2012;47:40-9.

[43] Romano F, Marocco L, Gustén J, Joppolo CM. Numerical and experimental analysis of airborne particles control in an operating theater. Building and Environment. 2015;89:369-79.

[44] Hinds WC. Aerosol technology: properties, behavior, and measurement of airborne particles. New York, Wiley-Interscience, 1982 442 p. 1982;1.

[45] Xu Y, Yang X, Yang C, Srebric J. Contaminant dispersion with personal displacement ventilation, Part I: Base case study. Building and Environment. 2009;44:2121-8.

[46] Chen F, Simon C, Lai AC. Modeling particle distribution and deposition in indoor environments with a new drift–flux model. Atmospheric Environment. 2006;40:357-67.

[47] Fanger PO. Thermal comfort. Analysis and applications in environmental engineering. Thermal comfort Analysis and applications in environmental engineering. 1970.

[48] Horikiri K, Yao Y, Yao J. Numerical optimisation of thermal comfort improvement for indoor environment with occupants and furniture. Energy and Buildings. 2015;88:303-15.

[49] ISO7730. Moderate thermal environments-determination of the PMV-PDD indices and specification of the conditions for thermal comfort. 1994.

[50] Lian Z, Wang H. Experimental study of factors that affect thermal comfort in an upward-displacement air-conditioned room. HVAC&R Research. 2002;8:191-200.

[51] Rees S, McGuirk J, Haves P. Numerical investigation of transient buoyant flow in a room with a displacement ventilation and chilled ceiling system. International Journal of Heat and Mass transfer. 2001;44:3067-80.

[52] Fathollahzadeh MH, Heidarinejad G, Pasdarshahri H. Prediction of thermal comfort, IAQ, and energy consumption in a dense occupancy environment with the under floor air distribution system. Building and Environment. 2015;90:96-104.

[53] Heidarinejad G, Fathollahzadeh MH, Pasdarshahri H. Effects of return air vent height on energy consumption, thermal comfort conditions and indoor air quality in an under floor air distribution system. Energy and Buildings. 2015;97:155-61.

[54] Lin Y, Xu Z. Buoyancy-driven flows by a heat source at different levels. International Journal of Heat and Mass Transfer. 2013;58:312-21.

[55] Serrano-Arellano J, Xamán J, Álvarez G. Optimum ventilation based on the ventilation effectiveness for temperature and CO_2 distribution in ventilated cavities. International Journal of Heat and Mass Transfer. 2013;62:9-21.